

ROTATION INVARIANT TOPOLOGY CODING OF 2D AND 3D OBJECTS USING MORSE THEORY

Sajjad Baloch[†], Hamid Krim[†], Irina Kogan[‡], and Dmitry Zenkov[‡]
North Carolina State University, Raleigh, NC 27695

ABSTRACT

In this paper, we propose a numerical algorithm for extracting the topology of a three-dimensional object (2 dimensional surface) embedded in a three-dimensional space \mathbb{R}^3 . The method is based on capturing the topology of a modified Reeb graph by tracking the critical points of a distance function. As such, the approach employs Morse theory in the study of translation, rotation, and scale invariant skeletal graphs. The latter are useful in the representation and classification of objects in \mathbb{R}^3 .

1. INTRODUCTION

Topology is an important attribute of 3D objects which describes how different parts of an object surface are connected to each other. Two objects have the same topology if one can be morphed into the other with no tearing or gluing. Geometry, on the other hand, represents the relative position of points on the surface. For example, a camel and a frog have different geometric properties whereas topologically they are the same.

In this paper, we propose a novel algorithm that computes a skeletal graph and thus captures the topology of a 3D object. Simultaneously, the algorithm extracts the geometric properties of the object. The proposed encoding of the topology and geometry of an object is sufficiently complete for classification/recognition applications. We also provide some results which show that the technique is applicable to 2D objects as well.

The paper is organized as follows: We start with a brief overview of Morse theory in Section 2 followed by a literature review in Section 3. The proposed method is exposed in Section 4, and some experimental results are shown in Section 5.

2. AN OVERVIEW OF MORSE THEORY

In this paper, a 3D object to be analyzed is replaced with its 2D boundary, which is assumed to be a compact two-dimensional manifold embedded in \mathbb{R}^3 . It is further assumed that all manifolds of interest are smooth.

Morse theory [5], [1], [4] relates the topology of a smooth manifold and the number of critical points of a *Morse function* (see the definition below) on this manifold.

A k -dimensional manifold \mathcal{M} may be locally parameterized as

$$\phi : \Omega \rightarrow \mathcal{M},$$

that is, $\Omega \ni u \mapsto \phi(u) \in \mathcal{M}$, where an open connected set $\Omega \subset \mathbb{R}^k$ represents the parameter space. Let $f : \mathcal{M} \rightarrow \mathbb{R}$ be a

[†]Department of Electrical and Computer Engineering.

[‡]Department of Mathematics.

This work was supported by AFOSR F49620-98-1-0190 and NSF CCR-9984067 grants.

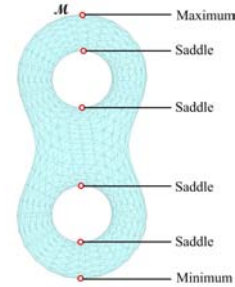


Fig. 1. Manifold \mathcal{M} and the critical points of the height function.

real-valued function defined on \mathcal{M} . By definition, f is smooth if the composition $f \circ \phi : \Omega \rightarrow \mathbb{R}$ is smooth for each local parameterization of \mathcal{M} . A point $x = \phi(u) \in \mathcal{M}$ is called a *critical point* of f if the gradient of $f \circ \phi$ vanishes at u , i.e., $\nabla f \circ \phi(u) = 0$. The critical point $x \in \mathcal{M}$ is called *non-degenerate* if the Hessian $\nabla^2 f \circ \phi(u)$ is non-singular at u .¹ The *Morse Lemma* states that there exists a parameterization of a neighborhood of a non-degenerate critical point of f in which $f \circ \phi$ is a quadratic form. The number of negative eigenvalues of the matrix of this quadratic form is called the *index of the critical point*. For a smooth function on a two-dimensional manifold \mathcal{M} , the three possible types of non-degenerate critical points are the local minimum (index 0), saddle point (index 1), and local maximum (index 2).

Definition 2.1: (Morse function) A smooth function $f : \mathcal{M} \rightarrow \mathbb{R}$ on a smooth manifold \mathcal{M} is called a Morse function if all of its critical points are non-degenerate.

Following are the basic properties of critical points of Morse functions:

- Critical points of a Morse function are isolated.
- The number of critical points of a Morse function is stable, i.e., a small perturbation of the function neither creates nor destroys critical points.
- A Morse function defined on a compact manifold has finitely many critical points.

It should be noted that the type and number of critical points allow one to identify the topological structure of \mathcal{M} .

In this paper, we concentrate on the study of 2D surfaces embedded in \mathbb{R}^3 . The points of \mathbb{R}^3 are represented by their position vectors, which are typed in bold. The parameter space Ω is two-dimensional, and points in Ω are written as (u, v) . Thus, if \mathbf{x} lies on the surface, we write $\mathbf{x} = \mathbf{x}(u, v)$.

Example 2.2: (Height function) The height function defined on a compact surface $\mathcal{M} \subset \mathbb{R}^3$ is a real valued function $h :$

¹This definition is independent of the choice of the local parameterization in the neighborhood of the critical point.

$\mathcal{M} \rightarrow \mathbb{R}$ such that $h(x, y, z) = z, \forall (x, y, z) \in \mathcal{M}$. If \mathcal{M} is a sphere S^2 , h has two non-degenerate critical points: a minimum at the south pole and a maximum at the north pole. Thus $h: S^2 \rightarrow \mathbb{R}$ is a Morse function.

Fig. 1 illustrates critical points of the height function defined on a double torus which correspond to the minimum, the maximum, and the saddle points.

3. PREVIOUS WORK

The use of the height function for topological analysis of manifolds was proposed by Reeb [6]. Shinagawa *et al.* [7] presented an algorithm for computing Reeb graphs. Although computationally simple, height function based Reeb graphs are not invariant with respect to rotations. As a remedy, Lazarus *et al.* [3] proposed skeletonization based on the geodesic distance from a manually chosen *source point* and called the graphs obtained this way the *level set diagrams*. Hilaga *et al.* [2] extended this approach by eliminating the need for manual selection of a source point and proposing a matching algorithm based on multiresolution Reeb graphs. Although this achieved rotational invariance, the algorithm became computationally intensive.

The approach proposed in this paper obtains rotation invariant skeletal graphs. In addition, the algorithm itself is computationally simple and resembles the algorithm for computing the height function-based Reeb graphs. We remark that the invariance with respect to rotations results from the use of the distance function in our analysis.

4. PROPOSED APPROACH

Consider the distance function $d: \mathbf{p} \mapsto \|\mathbf{p}\|$ in \mathbb{R}^3 . Given a generic surface $\mathcal{M} \subset \mathbb{R}^3$, the restriction of the distance function on \mathcal{M} ,

$$d: \mathcal{M} \rightarrow \mathbb{R}_+, \quad (1)$$

is a Morse function and can be used for constructing skeletal graphs.

To analyze and encode a compact surface using the Morse function (1), we start at the origin $d(\mathbf{p}) = 0$ and gradually increase the value of the distance function in K steps to a sufficiently large number which we denote b . The integer K is called the *resolution of the skeletal graph*. Making K larger increases the precision of captured structural changes in the level sets of the distance function. Recall that such changes occur only at critical level sets.

Since the level sets of d are concentric spheres, we find intersections of the manifold with spheres of radii R for all $R \in [0, b]$ and assign a node to each connected component in an intersection. This is illustrated in Fig.2. The skeletal graph may be described as the quotient space \mathcal{M}/\sim , where the equivalence relation \sim is defined below.

Definition 4.1: (Equivalence) We say that the points \mathbf{p} and \mathbf{q} on the surface are equivalent and write $\mathbf{p} \sim \mathbf{q}$ if and only if \mathbf{p} and \mathbf{q} belong to the same connected component of the level set of the function d .

Recall the definition of the quotient space: $\mathcal{M}/\sim := \{[\mathbf{p}] \mid \mathbf{p} \in \mathcal{M}\}$, where the equivalence class $[\mathbf{p}]$ of the point $\mathbf{p} \in \mathcal{M}$ is the set of all points $\mathbf{q} \in \mathcal{M}$ such that $\mathbf{q} \sim \mathbf{p}$.

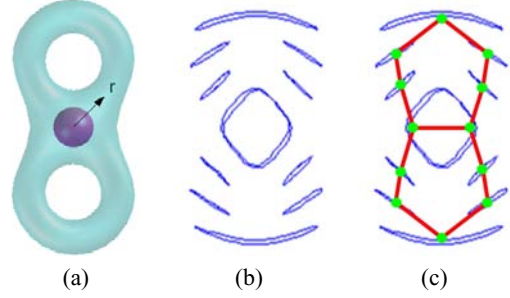


Fig. 2. Skeletal graph of a double torus: (a) The surface analysis with an evolving sphere; (b) Intersections of the spheres and the surface; (c) Node assignment in the graph.

Note that the function d given by Eq. (1) is not invariant with respect to translation and scaling. In order to have this invariance, we put the origin at the centroid $\boldsymbol{\mu}$ of the surface of interest and set

$$d_{\boldsymbol{\mu}}(\mathbf{p}) := \|\mathbf{p} - \boldsymbol{\mu}\|.$$

We then introduce the scaled distance function $\tilde{d}_{\boldsymbol{\mu}}$ by the formula

$$\tilde{d}_{\boldsymbol{\mu}}(\mathbf{p}) = \frac{d_{\boldsymbol{\mu}}(\mathbf{p}) - d_{\min}}{d_{\max} - d_{\min}}. \quad (2)$$

Proposition 4.2: (Invariance) The distance function given by Eq. (2) is rotation, translation, and scale invariant.

Proof: We will prove this statement for two-dimensional manifolds. Let $\boldsymbol{\mu} = (\mu_x, \mu_y, \mu_z)$ be the centroid of the manifold \mathcal{M} , and let \mathbf{p} be an arbitrary point on \mathcal{M} .

We first confirm that the function $d_{\boldsymbol{\mu}}$ is translational and rotational invariant. An arbitrary Euclidean transformation of \mathbb{R}^3 is given by $\mathbf{p} \mapsto A\mathbf{p} + \mathbf{b}$, where the vector \mathbf{b} represents the translation and the orthogonal matrix A represents the rotation. Since $\boldsymbol{\mu}$ undergoes the same transformation, we have

$$\begin{aligned} d_{A\boldsymbol{\mu} + \mathbf{b}}(A\mathbf{p} + \mathbf{b}) &= \|(A\mathbf{p} + \mathbf{b}) - (A\boldsymbol{\mu} + \mathbf{b})\| \\ &= \|A(\mathbf{p} - \boldsymbol{\mu})\| \\ &= \|\mathbf{p} - \boldsymbol{\mu}\| \\ &= d_{\boldsymbol{\mu}}(\mathbf{p}). \end{aligned}$$

Therefore, $\tilde{d}_{\boldsymbol{\mu}}$ is invariant with respect to rotations and translations in \mathbb{R}^3 .

Now if we scale the manifold by a factor of a , then

$$\begin{aligned} d_{\boldsymbol{\mu}}(a\mathbf{p}) &= \sqrt{(ax)^2 + (ay)^2 + (az)^2} \\ &= a\sqrt{x^2 + y^2 + z^2} \\ &= ad_{\boldsymbol{\mu}}(\mathbf{p}), \end{aligned}$$

and therefore,

$$\begin{aligned} \tilde{d}_{\boldsymbol{\mu}}(a\mathbf{p}) &= \frac{d_{\boldsymbol{\mu}}(a\mathbf{p}) - ad_{\min}}{ad_{\max} - ad_{\min}} \\ &= \frac{d_{\boldsymbol{\mu}}(\mathbf{p}) - d_{\min}}{d_{\max} - d_{\min}} \\ &= \tilde{d}_{\boldsymbol{\mu}}(\mathbf{p}). \end{aligned}$$

■

4.1. Equations for the Critical Points of the Distance Function

Assume that the surface \mathcal{M} is locally parameterized as a graph, i.e., $\mathbf{p} = (u, v, g(u, v))$, and that the centroid is located at the origin. The distance function $d(x, y, z) = \sqrt{x^2 + y^2 + z^2}$ restricted to \mathcal{M} reads

$$\tilde{d}(u, v) = d|_{\mathcal{M}} = \sqrt{u^2 + v^2 + g^2(u, v)}.$$

The partial derivatives of \tilde{d} are

$$\frac{\partial \tilde{d}}{\partial u} = \frac{2u + 2gg_u}{2\sqrt{u^2 + v^2 + g^2(u, v)}}$$

$$\frac{\partial \tilde{d}}{\partial v} = \frac{2v + 2gg_v}{2\sqrt{u^2 + v^2 + g^2(u, v)}}.$$

At a critical point the partial derivatives of \tilde{d} vanish. Therefore the critical points of the distance function on the surface \mathcal{M} are the solutions of the system

$$g_u(u, v) + \frac{u}{g(u, v)} = 0,$$

$$g_v(u, v) + \frac{v}{g(u, v)} = 0.$$

4.2. The Algorithm

The algorithm for computing extended Reeb graphs is illustrated in Fig. 3 and proceeds as follows:

- Find the centroid of the surface \mathcal{M} as the arithmetic mean of the vertices of the triangulated mesh and place the origin at the centroid
- Find d_{\max} , the maximum distance from the centroid to \mathcal{M}
- Given K , define:

$$r_k := k \frac{d_{\max}}{K}, \quad k = 1, \dots, K$$

- Generate the spheres \mathcal{S}_1 and \mathcal{S}_2 with radii $R = r_1$ and $R = r_2$, respectively
- Find $\mathcal{M}_p = \mathcal{M} \cap (\lfloor \mathcal{S}_1 \rfloor \cap \lceil \mathcal{S}_2 \rceil)$, where $\lceil \cdot \rceil$ and $\lfloor \cdot \rfloor$ identify the interior and exterior of a closed surface; \mathcal{M}_p is, therefore, the part of \mathcal{M} that lies between \mathcal{S}_1 and \mathcal{S}_2
- Assign a node $N_{\mathcal{M}_p}$ to each connected component \mathcal{M}_p of $\tilde{\mathcal{M}}_p$ at the centroid of \mathcal{M}_p
- For $k = 3$ to K
 - Generate the “current” sphere \mathcal{S}_k with radius $R = r_k$
 - Find $\tilde{\mathcal{M}}_c = \mathcal{M} \cap (\lfloor \mathcal{S}_{k-1} \rfloor \cap \lceil \mathcal{S}_k \rceil)$. Hence, $\tilde{\mathcal{M}}_c$ is the portion of \mathcal{M} that lies in between \mathcal{S}_{k-1} and \mathcal{S}_k
 - Find the connected components \mathcal{M}_c of $\tilde{\mathcal{M}}_c$
 - For each $\mathcal{M}_c \in \tilde{\mathcal{M}}_c$ do
 - * Assign a node $N_{\mathcal{M}_c}$ at the centroid of \mathcal{M}_c
 - * Find the connected region $\mathcal{M}_p \in \tilde{\mathcal{M}}_p$ such that $\mathcal{M}_c \cup \mathcal{M}_p$ is a single connected region. Add an edge between $N_{\mathcal{M}_c}$ and $N_{\mathcal{M}_p}$
 - end for
 - $\tilde{\mathcal{M}}_p = \tilde{\mathcal{M}}_c$
- end for.

4.3. Application to 2D Objects

The algorithm given in Section 4.2 is applicable to planar curves with a slight modification. The curve is now scanned by an evolving circle, whose intersections with the curve are arcs instead of closed curves. Results are presented in Section 5.

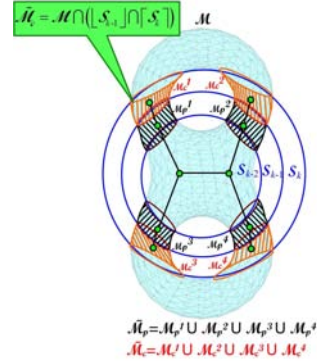


Fig. 3. Skeletonization of a surface \mathcal{M} in \mathbb{R}^3 .

5. EXPERIMENTAL RESULTS

5.1. 3D Objects

Extended Reeb graphs for several 3D objects are given in Figs. 4 through 7. Fig. 8 illustrates rotational invariance of the proposed technique.

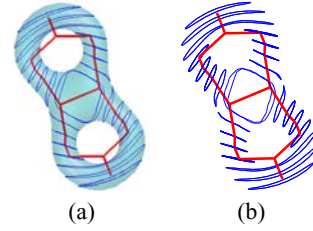


Fig. 4. Extended Reeb graph and level curves for a double torus.

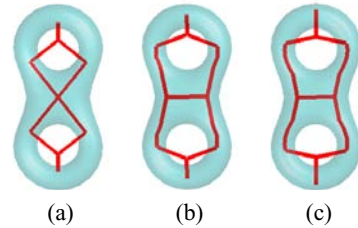


Fig. 5. Extended Reeb graphs for a double torus: (a) $K = 4$; (b) $K = 8$; (c) $K = 16$.

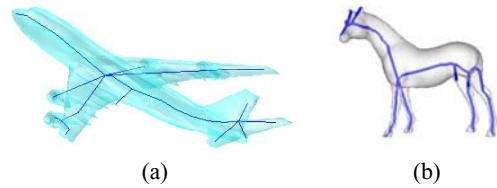


Fig. 6. Extended Reeb graphs: (a) An airplane; (b) A horse.

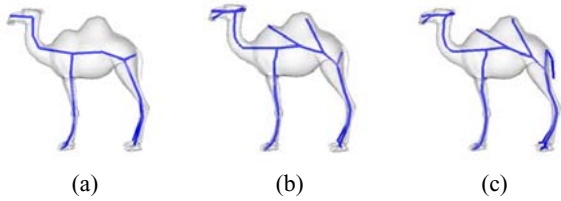


Fig. 7. Extended Reeb graphs for a camel: (a) $K = 8$; (b) $K = 16$; (c) $K = 32$.

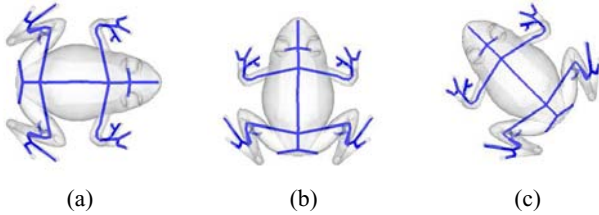


Fig. 8. Rotational invariance of extended Reeb graph: (a) No rotation; (b) Rotation by $\pi/2$; (c) Rotation by $3\pi/4$.

5.2. 2D Objects

Extended Reeb graphs of 2D objects are given in Figs. 9 through 12.

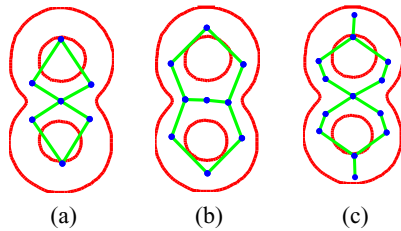


Fig. 9. Skeletonization of an eight shape: (a) $K = 4$; (b) $K = 5$; (c) $K = 7$.

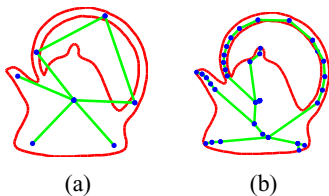


Fig. 10. Skeletonization of a kettle: (a) $K = 4$; (b) $K = 16$.

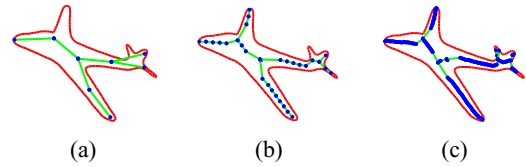


Fig. 11. Skeletonization of an airplane: (a) $K = 4$; (b) $K = 16$; (c) $K = 64$.

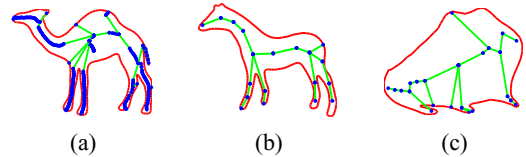


Fig. 12. Skeletonization: (a) Camel $K = 64$; (b) Horse $K = 8$; (c) Frog $K = 16$.

6. CONCLUSIONS

In this paper, we have presented an algorithm for capturing the topology of 3D objects using the distance function based Reeb graphs. The distance function based Reeb graphs have shown to be rotation, translation, and scale invariant. The technique has been applied to 2D objects as well. The algorithm we proposed in this paper can be used for object recognition through graph matching.

REFERENCES

- [1] M. D. Carmo, *Differential Geometry of Curves and Surfaces*, Prentice-Hall, New Jersey, 1976.
- [2] M. Hilaga, Y. Shinagawa, T. Kohmura, and T. L. Kunii, "Topology Matching for Fully Automatic Similarity Estimation of 3D Shapes", *Proc. SIGGRAPH*, pp. 203–212, August 2001.
- [3] F. Lazarus, and A. Verroust, "Level set diagrams of polyhedral objects", *Proc. Fifth ACM symposium on Solid Modeling and Applications*, pp. 130–140, June 1999.
- [4] Y. Matsumoto, *An Introduction to Morse Theory*, American Mathematical Society, 1997.
- [5] J. Milnor, *Morse Theory*, Princeton University Press, Princeton, NJ, 1963.
- [6] G. Reeb, "Sur les points singuliers d'une forme de pfaff complètement intégrable ou d'une fonction numérique", *Comptes Rendus de L'Académie ses Séances*, Paris, 222, pp. 847–849, 1946.
- [7] Y. Shinagawa, and T. L. Kunii, "Constructing a Reeb graph automatically from cross sections", *IEEE Computer Graphics and Applications*, 11(6), pp. 44–51, November 1991.